Research Square

Preprints are preliminary reports that have not undergone peer review.
They should not be considered conclusive, used to inform clinical practice,
or referenced by the media as validated information.

Facile development of multifunctional photoluminescent linen fabrics for high performance textile applications

Esraa Ahmed
Helwan University
Dalia Maamoun
Helwan University
Talaat M. Hassan
Helwan University
Tawfik Khattab (tkhattab@kent.edu)
National Research Centre

Research Article

Keywords: Linen fabric, Pad-dry-cure, Long-persistent photoluminescence, Hydrophobic, Fame-resistant

Posted Date: April 7th, 2022

DOI: https://doi.org/10.21203/rs.3.rs-1516820/v1

License: This work is licensed under a Creative Commons Attribution 4.0 International License.
Read Full License

Abstract

Linen fibers were coated with a luminous, flame-retardant, and hydrophobic smart nanocomposite utilizing the pad-dry-curing process. Ecologically-friendly ammonium polyphosphate and lanthanide-activated strontium aluminum oxide (LSAO) nanoparticles were immobilized into linen fabric using the eco-friendly RTV silicone rubber. Scanning electron microscopy (SEM), energy-dispersive X-ray (EDX), X-ray fluorescence (XRF) spectroscopy, Fourier-transform infrared (FTIR) spectroscopy, and transmission electron microscopy (TEM) were employed to examine the morphological characteristics and elemental compositions of LSAO nanoparticles and treated linen textiles. The self-extinguishing properties of the treated linen textiles were tested for their fire-resistance. After 24 washing cycles, the coated linen samples retained their flame-retardant properties. The treated linen's superhydrophobicity rose in direct proportion to the LSAO concentration. After being excited at 365 nm, the colorless luminescent film that was coated on linen surface gave out an emission wavelength of 519 nm. The photoluminescent linen was monitored to create a range of different colors, including off-white in daytime light and green under UV radiation, according to the CIE Lab colorimetric coordinates and photoluminescence spectra. Emission, excitation and lifetime spectral analysis of the treated linen revealed persistent phosphorescence. For mechanical and comfort evaluation, the coated linen textiles' bending length and air permeability were assessed. Excellent UV protection and enhanced antibacterial properties were found in the treated linens. Large-scale manufacturing of multipurpose technical fabrics, such as tents, might benefit from the current simple technique.

Highlights

- Multiple functional nanocomposite was pad-dry-cured into linen fabrics.
- Glow in the dark emission (>1 hour) with high photostability was achieved.
- Effective ultraviolet protection and superhydrophobicity were explored.
- Linen fabrics showed good mechanical and antimicrobial properties.
- Flame-retardant behavior was maintained against 24 washing cycles.

1. Introduction

When it comes to smart clothes, especially protective technical fabrics, the market is ripe with opportunity. Functional textiles produced for purposes other than aesthetics include antibacterial, superhydrophobic, and flame retardant materials. This kind of material is also known as "smart textiles" since it may change color or luminescence properties in response to external stimuli. Having long-lasting phosphorescence in textiles that light up in the dark is desired [1, 2]. Light is absorbed into the crystals of phosphorescence substances. The trap component in the phosphorescence compound then collects the light energy. Eventually, the photons of light that were trapped are released from the traps [3]. Strontium aluminates that are activated by rare earth elements have been employed in a number of applications, including emergency signs, safety textiles and photochromic ink [4]. Several phosphorescent pigments

have been described with their ability to develop a wide range of products with various emission colors, such as the greenish emission from $SrAl_2O_4:Eu^{2+},Dy^{3+}$ [5]; bluish emission from $CaAl_2O_4:Eu^{2+},Nd^{3+}$ [6]; and red emission from $Y_2O_2S:Eu^{3+},Mg^{2+},Ti^{4+}$ [7]. As a result of its high quantum efficiency, high recyclability, nonradioactivity, and good thermal, chemical and photostability, LSAO has long been considered a key long-lasting phosphor [8–10]. Hydrophobic surfaces could be created using a variety of techniques, including nanofibers, chemical etching, plasma, sol-gel, and lithography. However, those techniques have demonstrated difficulties such as slow and hard processing, and the requirements of trained personnel and sophisticated instruments [11]. Using the pad dry curing procedure to coat fabrics is a straightforward and cost-effective way to make useful outerwear. In transportation and packing, textiles' hydrophilicity tends to restrict their utility. Static contact angle of > 150° and sliding angle of < 10° are required for superhydrophobic materials [12, 13]. As a result, corrosion prevention, maritime industry, antifouling, and oil-water separation have all profited from the usage of superhydrophobic materials [14]. Using micro/nanoscale hierarchical materials, hydrophobic substrates with high surface roughness have been developed. Fluorine-based chemicals have been utilized to make hydrophobic materials. These compounds, on the other hand, have been proved to be costly and dangerous [15–17]. In recent years, the emphasis of research has shifted to environmentally benign compounds for superhydrophobic materials. Using a butynorate catalyst to ambient temperature vulcanize silicone rubber is an environmentally friendly polymerization. Chemical, heat, and age resistance are just a few of the properties of silicone rubber. Typical properties of silicone rubber include a low viscosity, high hardness, and low shrinking. It is utilized in aircraft, 3D printing, optics, and electronics [18–21].

Flame retardant treatment could be applied to flammable materials in order to limit the potential for damage caused by burning. Firefighters could slow and restrict the blazing process to perform rescue operations and help persons trapped in wildfires escape [22]. Different chemical agents have been developed to improve the resistance to flames in various products. Halogen-containing fire-retardant chemical agents have been demonstrated to emit poisonous gases [23] despite their widespread usage. Inorganic boron-containing flame retardants are not producible industrially because their matrices do not have sufficient binding ability. Phosphorus-bearing flame retardants, on the other hand, have long been acknowledged as environmentally friendly. In compliance with environmental regulations, phosphorus-based flame retardant chemicals create no toxic substances during the blazing process [24, 25]. The flame retardant performance could be improved by loading two or more types of organic-based phosphorus and nitrogen/phosphorus derived components into a product matrix. Fibers made of linen are more durable, have lower heat conductivity, are more absorbent, and dry faster than fibers made of cotton. Towels, napkins, tablecloths, and chair coverings are just some of many linen-based goods on today’s market. Until recently, linen was a cheap and plentiful commodity [26]. Compared to cotton fibers, it has a longer staple length. Because of its durable nature and low allergenic potential, linen is now one of the most popular fabrics for bed linens. Despite this, linen substrates have been limited in their application due to their intrinsic flammability, low water resistance, and microbial invasion [27]. When immobilizing superhydrophobic and photoluminescence agents into textile material, a variety of useful products for both garments as well as high-performance applications could be produced [28]. According

to literature, linen goods with photoluminescence, superhydrophobic, and fire-resistant properties have not been documented yet [29, 30]. It is possible to maintain the flame-retardant performance of linen for a longer time periods by imparting hydrophobicity to the treated linen, which allows linen to provide an improved protection value. Thus, photoluminescence, superhydrophobicity, and fire-resistant properties could be combined to boost the durability of the treated linen fabrics.

Herein, we describe the production of superhydrophobic, flame retardant and photoluminescent linen fabrics using the pad dry curing technology. Ammonium polyphosphate, LSAO nanoparticles, and silicone rubber were admixed together to provide a nanocomposite coating film for linen. Throughout the burning test, the as-coated linen fibers demonstrated superhydrophobic and photoluminescent properties, as well as the capacity to form a char layer during the burning period, exhibiting self-extinguishing qualities. After 24 washing cycles, the treated linen samples retain their self-extinguishing qualities. LSAO was employed as a photoluminescent agent, silicone rubber was employed as a superhydrophobic and crosslinking agent, and ammonium polyphosphate was used as the flame-retardant compound. The shape and diameter of the nanoscale pigment particles were inspected using TEM. The morphology and elemental contents of cured linen were studied using XRF, EDX, SEM, and FTIR. Significant differences in the characteristics of the treated linen substrates could be attributed to the quantity of LSAO nanoparticles. The water-repellent properties of the phosphor nanopowder were improved by increasing the quantity of LSAO nanopowder. The luminescence properties of the cured linen were evaluated using excitation, emission, decaying, and lifetime spectra. Comfort was evaluated by taking measurements of bend length and air permeability. Textiles could be finished using the current approach on a large scale without the need for costly technology, making it suited to mass-produce multiple-purpose clothes.

2. Experimental

2.1. Materials and reagents

The linen sample was supplied from Misr-Helwan for Spinning and Weaving (Egypt). Both bleaching and scouring of linen were carried out according to previously reported procedures [31]. To remove all waxes and impurities, the linen samples were scoured for 30 minutes in aqueous medium using 2 g/L of Na_2CO_3 and 2 g/L of Hostapal detergent (Clariant, Swiss) at a liquor ratio of 1:50. Afterwards, the materials were rinsed with water and air-dried. Ammonium polyphosphate (Exolit AP 422) was provided by Shandong Shi'an for Chemicals (China). Silicone rubber (Decoseal 25–40) was provided by ADMICO (Egypt). Toluene was provided by Merck (Egypt). Dysprosium oxide (Dy_2O_3), boric acid (H_3BO_3), aluminum oxide (Al_2O_3), strontium carboxylate ($SrCO_3$), and europium oxide (Eu_2O_3) were provided from Aldrich (Egypt). Aluminum strontium oxide activated with alkaline earth (europium and dysprosium oxide) was synthesized using the already well-proven high temperature solid state synthesis method [32]. Two mol of aluminum oxide, one mol of strontium carbonate, one mol of boric acid, one mol of dysprosium oxide, and one mol of europium oxide were combined in absolute ethanol (400 mL) to form a suspension. The admixture was dried at 90°C for 22 hours after being homogenized (25 kHz; 60 min).

Two hours of milling and three hours of sintering at 1300°C in a reduction carbon atmosphere were required to sinter the given powder. The generated residue was grinded and sieved to get phosphor microscale particles. Using the top-down technique [33], the phosphor microscale particles (10 g) were charged into a stainless steel tube (20 cm) positioned on a vibrating plate, where the LSAO nanoscale particles were generated using the ES80 Triple Roll Milling system. The stainless steel ball mill tube with the phosphor microparticles and the vibrating plate were collided for 24 hours with a silicon carbide ball that was 0.01 cm in diameter to provide the LSAO nanoscale particles.

2.2. Preparation of functional linens

A solution of RTV (10% w/v) in toluene was stirred for 60 minutes. This was followed by 60 minutes of stirring with 20% (w/v) of ammonium polyphosphate. A variety of LSAO concentrations were then added; 0, 0.5, 1, 2, 4, 6, 8, 10, 12, and 14% w/w, which were abbreviated with $LSAO_0$, $LSAO_1$, $LSAO_2$, $LSAO_3$, $LSAO_4$, $LSAO_5$, $LSAO_6$, $LSAO_7$, $LSAO_8$, and $LSAO_9$, respectively. Each solution was homogenized (25 kHz) for 30 minutes, and stirred for 30 min. The linen substrates (15 cm x 15 cm) were exposed to 15 min of immersion in the produced composites at room temperature. The fabrics were air-dried for an hour in order to remove the solvent entirely from the treated linen.

2.3. Methods and apparatus

2.3.1. Morphological and structural properties

LSAO's shape and size was determined by JEOL1230 TEM (Japan). An aqueous suspension of the phosphor powder was homogenized at 35 kHz for 15 minutes before being placed on a copper grid for TEM analysis. Quanta FEG250 SEM and TEAM EDS (Republic of Czech) were used to analyze the morphology and chemical contents of both treated and untreated linen textiles. The nanoparticle size on the linen fabric surface was measured using Image J program set up on SEM. The chemical compositions of both treated and untreated linen textiles were also determined by using AXIOS XRF. Nicolet Nexus 670 spectrophotometer (U.S.A.) was used to capture the transmission FT-IR (4000 – 400 cm^{-1}) spectral profiles.

2.3.1. Photoluminescence studies

JASCO FP6500 (Japan) was used for linen luminescence spectral analysis. To assess the decay time of the luminous linen fabric, a 150 W Xenon Arc lamp was utilized for 15 minutes of exposure. In order to capture the data in full darkness, the UV bulb had to be shut off. An ultraviolet light of 6 W was placed 10 cm above the fabric to evaluate the linen's reversibility. Lights were turned off for 90 minutes so that the cloth sample could be restored to its original condition. The technique outlined above was repeated numerous times, and the resulting emission spectrum profile was reported.

2.3.2. Colorimetric properties

The pad-dry-cured linen textiles were studied using color strength (*K/S*) and CIE Lab, where lightness from white(100) to dark(0), color ratio of green(-)/red(+), and color ratio of blue(-)/yellow(+) were represented

by L^*, a^* and b^*, respectively [34]. Photographs were taken with the Canon A710IS in three distinct lighting conditions: daytime light, UV rays, and total darkness.

2.3.3. Hydrophobic properties

The wettability time, and contact and sliding angles were determined by using Dataphysics OCA15EC (GmbH, Germany) [35]. All measurements were performed in accordance with the ASTM D-7334 standard technique. A double-sided adhesive tape was used to attach the linen cloth to a glass slide to make a flat sample.

2.3.4. Flammability and durability evaluation

The standard BS 5438 (1989) [36] technique was used to measure the char length ((mm)) of both uncoated and coated linen. In accordance with AATCC 61 (1989) [37], the linen textiles (15 cm x 15 cm) were subjected to washing cycles ranging from 2 to 24. Detergent (66 g; AATCC standard) was used to wash the samples at 40°C in an accelerated launder-o-meter washing machine. It took 45 minutes to wash one load of laundry. The durability was assessed by taking a measurement of the char length after each cycle.

2.3.5. Mechanical behavior

Using the Textest FX3300 and ASTM D737 as a standardized guide, we were able to get an accurate reading of the air permeability at 100 Pa [38]. Shirley Stiffness device was used to measure the bend length of uncoated and coated linen in both warp and weft directions [39] in accordance with the British standard 3356 (1961).

2.3.6. Ultraviolet shielding

UV blocking qualities of linen textiles were tested using the Ultraviolet Protection Factor. Transmittance 183 (2010) UVA standard approach was used to record it [40].

2.3.7. Antimicrobial properties

Escherichia coli, Staphylococcus aureus, and Candida albican were evaluated for antibacterial properties of the coated linen. The quantitative counting approach was done using the AATCC technique 100 (1999) [41].

3. Results And Discussion

3.1. Photoluminescence spectra

The LSAO nanoscale particles were applied to linen surface using the pad-dry-cure process. Figure 1 shows images of coated linen sample ($LSAO_7$) taken under daytime light, UV light (365 nm), and complete darkness. The colorimetric alterations ranging from white in daytime to green under UV rays and greenish-yellow in complete darkness were caused by these different exposure environmental

conditions. Organic matrix (RTV) was employed as a bulk material to hold LSAO and Exolit on cloth. Phosphorescent film prepared by trapping LSAO nanoparticles and Exolit in RTV matrix showed identical photoluminescence activity as a powder of LSAO [32]. Fibers that are hydrophobic, flame-resistant, and long-persistent phosphorescent have been developed for the first time in this study.

Spectra of excitation and phosphorescence for the coated linen textiles are shown in Figs. 2–3. Reversible phosphorescence was monitored in all of the UV-irradiated samples. Even after switching off the ultraviolet supply, the coated linen samples continued to emit light and displayed long-lasting phosphorescent emission with increasing LSAO concentration (from $LSAO_3$ to $LSAO_9$). $LSAO_1$ and $LSAO_2$, on the other hand, displayed just fluorescence with no emission peaks apparent directly after the UV light was turned off. Thus, linen substrates treated with LSAO similar to or higher than $LSAO_3$ were the best candidates to promote long-lasting phosphorescence. Figure 3 shows a strong and wide emission band as a consequence of the 519 nm emission wavelength.

Lifetimes ranging from 0.9324 to 21744 ms for the linen fabrics with the lowest and highest LSAO concentrations were observed, suggesting a proportional relationship between LSAO ratio and lifetime of the coated sample (Fig. 4). The RTV/Exolit/LSAO nanocomposite was found to extend the lifetime of the linen photoluminescence with increasing the LSAO concentration. When the LSAO concentration was raised, the coated linen samples showed an increase in the emission intensity band. The lifetime curve was not linear as a function of time. Although the first stage of the lifetime curve was marked by a rapid drop, the second stage was marked by slower decline. In long-persistent phosphors, Dy^{3+} and Eu^{2+} have been used as traps to lengthen the phosphorescence time period. The density of traps affects the phosphorescence emission, whereas the depth of imprisoned photons has an effect on the persistence of the light emission.

Thus, the luminous linen fibers continue to emit light in the dark. The LSAO phosphorescence is caused by the Eu(II) $4f^6 5D^1 \leftrightarrow 4f^7$ transition, which has been previously reported [8]. Dy(III) and Eu(III) did not show any identifiable emission bands in the spectrum. This indicates that the photons stored by Dy^{3+} have been transferred to Eu^{2+}, and that the trivalent europium cations have been totally swapped to their divalent counterparts. The excitation spectroscopy revealed a broad range of spectrum (390–700 nm), which allows for a broad range of electromagnetic spectrum absorption. The co-doping with Dy(III) results in the release of hole traps when UV light is turned off. A long-lasting glow could be seen when Eu(II) receives the discharged holes and returns to the ground state. Using multiple cycles of UV irradiation/darkness as indicated in Fig. 5, the reversibility of treated linen was investigated. First, it was irradiated with UV for 10 min, and left in darkness for 1.5 hour to exhaust the energy stored in the pigment phosphor. Phosphorescence intensity was measured after each cycle to show that the material was highly photostable.

3.2. Morphological properties

In order to create flame- and water-resistant photoluminescent smart linen textiles, a silicone rubber nanocomposite comprising the ammonium polyphosphate flame retardant and the luminescent LSAO nanoparticles was used. Both LSAO nanoparticles and ammonium polyphosphate were attached to linen fabric by RTV matrix, which introduces a superhydrophobic layer. Nanoscale particles with diameters between 17 and 29 nm (Fig. 6) were produced by applying the top-down technique on the LSAO microscale particles synthesized by the solid state high temperature method [32, 33]. In order to produce a transparent layer onto linen surface, it was necessary to assure the effective dispersion of the phosphor nanoparticles throughout the RTV matrix before coating onto linen surface. Different concentrations of the phosphor nanoparticles were then dispersed with a mixture of silicone rubber and ammonium polyphosphate in toluene. Each composite was pad-dry-cured onto linen at ambient conditions. The produced linen samples were coated with a nanocomposite of RTV as a crosslinking and hydrophobic substance, ammonium polyphosphate as a flame retardant agent, and LSAO nanoparticles as a photoluminescent agent.

We employed WD-XRF, SEM, EDX, and FTIR to examine the morphologies and elemental structure properties of coatings on linen fibers. Analysis of linen's morphological features revealed its luminous, flame-resistant, and water-repellent capabilities. Figure 7 shows SEM images of $LSAO_1$ and $LSAO_9$. The functional properties of the coated linen could be attributed to a uniformly distributed layer of nano-hierarchical structures on linen fibers to result in an increase in surface roughness. As a consequence, the coated linen fibers were shown to be more water-repellent than $LSAO_0$. EDS was employed to assess the elemental contents of the treated linen fibers as shown in Table 1. Homogeneous dispersion of RTV/Exolit/LSAO nanocomposite was confirmed by the chemical content of the treated linen fibers at three points on linen surface. In the carbohydrate cellulose polymer that makes up linen, oxygen (O) and carbon (C) are the major constituents detected by EDX. EDX also detected silicone (Si) and phosphorus (P) with lower concentrations due to RTV and ammonium polyphosphate, respectively. The presence of LSAO nanoparticles were the reason for the detection of other elements at lower concentrations, including Sr, Al, Eu, and Dy. The chemical composition of the treated linen textiles was also determined by XRF, as indicated in Table 2. EDX is an accurate technique to determine the elemental concentrations at very low concentration levels. When it comes to WD-XRF, the detection limit is more than 10 mg/kg [42]. WD-XRF was able to offer a partial identification of the elemental composition, including silicone, strontium, and aluminum, since some elements (Dy and Eu) on the treated cloth surface are present in very low amounts. Due to their very low amounts, WD-XRF was unable to make an identification of Dy and Eu. According to EDX and WD-XRF analysis, the molar ratios employed to prepare the LSAO and RTV/Exolit/LSAO nanocomposites were similar to those detected by EDX and XRF on the treated linen fibers.

Table 1
EDX analysis (wt%) of blank and treated linen at three sites (S_1, S_2 and S_3).

LSAO (wt%)		C	O	Si	P	Al	Sr	Eu	Dy
$LSAO_0$		62.58	37.42	0	0	0	0	0	0
$LSAO_1$	S_1	43.75	23.13	20.80	9.17	1.70	0.98	0.29	0.18
	S_2	44.41	23.63	21.09	9.50	1.41	0.84	0.21	0.09
	S_3	44.21	23.33	20.36	9.24	1.60	0.92	0.24	0.10
$LSAO_7$	S_1	39.90	30.35	15.71	5.13	4.83	2.99	0.60	0.49
	S_2	40.54	30.84	15.85	5.54	4.55	2.73	0.65	0.48
	S_3	40.39	30.51	15.17	5.23	4.75	2.91	0.62	0.42
$LSAO_9$	S_1	37.52	33.52	13.81	4.36	5.61	3.71	0.79	0.68
	S_2	38.15	33.95	14.12	4.67	5.43	3.45	0.85	0.56
	S_3	38.10	33.32	13.34	4.76	5.53	3.63	0.82	0.50

Table 2
XRF analysis of elemental contents (wt%) in both blank and treated linen.

Elements	$LSAO_1$	$LSAO_7$	$LSAO_9$
Al	4.60	19.72	26.38
Sr	1.96	11.53	14.70
Si	93.44	68.75	57.92

Inspection of the linen fabric functional substituents was carried out using FTIR spectral analysis. Blank linen showed typical absorbance peaks at 3358 cm^{-1} owing to hydroxyl (OH) stretch vibration, 2912 cm^{-1} due to stretching alkyl CH, 1033 cm^{-1} attributed to ether (C-O) stretch vibration, and 1462 cm^{-1} owing to alkyl CH bending vibrations. Treatment with the alkyl-rich RTV boosted the aliphatic CH's bending and stretching band intensities. The peak intensity of the OH stretch vibration was also demonstrated to decrease. The NH_4^+ substituent of the Exolit AP 422 flame retardant was monitored at 2912 and 1462 cm^{-1}. The peaks of P-O-P, P-O, and P-OH were detected at 1159, 1322, and 1560 cm^{-1}, respectively. The absorbance of 571 cm^{-1} was ascribed to Si-O bend vibration. Neither the measured bands nor their intensities changed much, indicating an entirely effective coating of linen fibers with a thin functional layer.

3.3. Hydrophobicity screening

The hydrophobic screening characteristics of the treated linen textiles were evaluated as shown in Table 3 and Fig. 8. A thin RTV/Exolit/LSAO layer was applied onto the fibrous linen surface. The RTV/Exolit/LSAO nanocomposite was found to create rougher surfaces by filling in the crevices and gaps between the linen fibrous threads. Due to its great wettability, the contact angle of $LSAO_0$ was unable to be determined (0°). The $LSAO_1$ treated linen has a considerably improved contact angle of 147.1°. When the LSAO ratio is increased, the contact angle increases dramatically from 147.1° ($LSAO_1$) to 153.7° ($LSAO_7$). The static contact angle decreased again from 153.7° ($LSAO_7$) to 152.9° ($LSAO_9$) when the amount of LSAO was raised further. The surface roughness increases with increasing concentrations of LSAO nanoparticles on the fabric's surface [43]. This could be countered, however, by decreasing the distance between the LSAO nanoparticles as their concentration becomes much higher. Thus, the surface roughness was adversely affected, resulting in reduced static contact angles [44]. LSAO nanoscale particles were put between fibers to give a smoother surface. Therefore, the surface roughness decreased by using a higher concentration of LSAO nanoparticles more than $LSAO_7$. Nanocomposites with $LSAO_7$ as their ideal total LSAO content could be deemed optimal in this regard. Fabrics with and without RTV/Exolit/LSAO treatment were tested for their sliding angles. With an increase in LSAO, linen's hydrophobicity was shown to rise, resulting to a substantially greater increase in wettability time than $LSAO_0$ (6 s). Because it doesn't need the use of sophisticated instruments or procedures, the current technique could be defined as a simple and cheap technique to present a hydrophobic surface. Thus, the current simple technique could be utilized to manufacture glow in the dark linen goods for a range of purposes, including tents and other protective materials. As a result of their hydrophobic properties, silicone-coated fibers are also capable of permeating oil while retaining water.

Table 3
Hydrophobicity screening of treated linen.

Fabric	Contact angle (°)	Sliding angle (°)	Wettability time (min.)
$LSAO_1$	147.1	12	45
$LSAO_2$	147.6	12	55
$LSAO_3$	148.3	12	> 60
$LSAO_4$	149.7	11	> 60
$LSAO_5$	151.2	10	> 60
$LSAO_6$	152.8	10	> 60
$LSAO_7$	153.7	9	> 60
$LSAO_8$	153.4	8	> 60
$LSAO_9$	152.9	8	> 60

3.4. Fire-retardant performance

The untreated linen failed the flame test because it was entirely burnt (Table 4). The flame retardant properties of the coated linen were remarkable, with the course of the fire being monitored and ceasing immediately when the fire source was relocated away from linen. The char length of the coated linen dropped little as the LSAO ratio rose. In order to improve the fire resistance, ammonium polyphosphate was cross-linked with silicone rubber on the fabric surface. The damaged char length was lowered from 48 mm to 41 mm by increasing the LSAO ratio from $LSAO_0$ to $LSAO_6$. However, increasing the LSAO ratio from $LSAO_6$ to $LSAO_9$ had almost no effect on the char length. As an environmentally benign and formaldehyde-free alternative to Pyrovatex-based flame retardants, ammonium polyphosphate has set to take their place. Thus, it is possible to reduce formaldehyde emissions from Pyrovatex using the current technology.

Table 4
Effect of LSAO concentration on linen flammability.

Fabric	Char length (mm)	Char width (mm)
Untreated linen	completely burnt	
$LSAO_0$	48	17
$LSAO_1$	48	17
$LSAO_2$	48	17
$LSAO_3$	47	17
$LSAO_4$	45	18
$LSAO_5$	42	18
$LSAO_6$	41	17
$LSAO_7$	41	18
$LSAO_8$	41	18
$LSAO_9$	40	18

The washability of the flame retardant linen sample ($LSAO_7$) was investigated. RTV was used as a trapping bulk to attach LSAO nanoparticles and ammonium polyphosphate to the cloth surface.

The char length was recorded after each washing cycle, as shown in Fig. 9. The char length increased throughout the course of 24 washes. However, the sample was found to be entirely burned after 24 laundry cycle.

3.5. Antimicrobial and ultraviolet shielding

E. coli, S. aureus, and C. albicans were tested using the plate agar count method [41]. An increase in the antibacterial activity was detected as a result of the addition of LSAO as summarized in Table 5. As the concentration of LSAO increased, the antibacterial activity of the treated linen improved, ranging from poor to fair and excellent. The ultraviolet protection factor (UPF) was used to examine the treated linen's UV blocking capacity at different LSAO concentrations, as indicated in Table 5. The UV blocking enhancement of the coated linen textiles with an increased LSAO ratio on the fabric surface was found to be explained by the increased ultraviolet absorption of the LSAO pigment due to its electronic structure.

Table 5
Antimicrobial (Microbial Reduction %) and ultraviolet protection of linen fabrics.

LSAO (wt%)	*E. coli*	*S. aureus*	*C. albicans*	UPF
$LSAO_0$	----	----	----	77
$LSAO_1$	21 ± 1.1	19 ± 1.3	----	185
$LSAO_2$	23 ± 1.0	20 ± 1.3	----	227
$LSAO_3$	28 ± 1.0	25 ± 1.0	----	254
$LSAO_4$	35 ± 1.0	31 ± 1.4	----	273
$LSAO_5$	41 ± 1.5	36 ± 1.0	9 ± 1.3	338
$LSAO_6$	45 ± 1.0	40 ± 1.0	9 ± 1.1	385
$LSAO_7$	46 ± 1.0	41 ± 1.4	9 ± 1.7	440
$LSAO_8$	48 ± 1.5	41 ± 1.6	9 ± 1.0	471
$LSAO_9$	48 ± 1.1	42 ± 1.0	9 ± 1.5	493

3.6. Mechanical properties

Using the pad dry curing technique, the main purpose is to produce a linen surface that is water-repellent while yet enabling the fabric to breathe and move freely. The physical characteristics of the fabric were significantly influenced by the application of RTV/Exolit/LSAO nanocomposites utilizing the pad dry cure process. Bending length and air-permeability screening findings are summarized in Table 6. There were no noticeable changes in air permeability when the LSAO concentration was raised compared to $LSAO_0$. It was found that the LSAO-treated linen exhibited slightly higher bending lengths compared to the untreated linen. Using the CIE Lab coordinates, the RTV/Exolit/LSAO layer influence on the color of the coated linen was evaluated as shown in Table 6. With the addition of LSAO, the coated linen exhibited a little drop in L^*. After increasing the amount of LSAO, there was a little change in the a^* and b^* values,

which indicated the formation of a transparent nanocomposite film on linen. The intrinsic characteristics of the treated linen were not considerably affected by the deposited superhydrophobic, flame-retardant and photoluminescent layer.

Table 6
Mechanical properties of both treated and untreated linen.

Fabric	Bend length (cm)		Permeability to air ($cm^3.cm^{-2}.s^{-1}$)
	weft	warp	
$LSAO_0$	4.51	5.12	40.63
$LSAO_1$	4.88	5.29	40.21
$LSAO_2$	5.06	5.48	39.83
$LSAO_3$	5.32	5.79	39.29
$LSAO_4$	5.57	5.98	38.89
$LSAO_5$	5.75	6.10	38.63
$LSAO_6$	5.96	6.38	38.24
$LSAO_7$	6.20	6.68	37.89
$LSAO_8$	6.38	6.97	37.55
$LSAO_9$	6.44	7.21	37.32

Table 6
Colorimetric screening of $LSAO_0$ and coated linen.

Fabric	L*	a*	b*
$LSAO_0$	87.80	-2.04	0.70
$LSAO_1$	86.55	-1.86	0.94
$LSAO_2$	86.06	-1.61	1.17
$LSAO_3$	85.35	-1.34	1.41
$LSAO_4$	84.45	-1.21	1.74
$LSAO_5$	82.42	-1.05	2.07
$LSAO_6$	82.03	-1.09	2.31
$LSAO_7$	81.74	-0.98	2.59
$LSAO_8$	81.63	-0.79	2.82
$LSAO_9$	81.16	-0.65	3.18

4. Conclusion

For the production of multipurpose linen textiles, the pad-dry-cure coating method was used. Antimicrobial, photoluminescent and UV protective properties were achieved by using rare earth doped aluminate. As a fire-retardant agent, we turned to the environmentally friendly organic ammonium polyphosphate. Eco-friendly RTV was used as both a hydrophobic agent and a bulk layer to contain both of illuminating phosphor and fire-resistant chemical agents on the linen fabric's surface. The fundamental features of linen, such as air permeability and flexibility, were maintained unaffected when the lanthanide doped aluminum strontium oxide is immobilized on its surface. In order to study the LSAO nanoparticles' morphology, TEM was utilized to indicate particle diameters of 17–29 nm. The morphology, elemental content and emission spectra of the treated linen were all investigated in detail. SEM, EDX, FT-IR, and XRF were employed to evaluate the surface morphologies of the treated linen. The flame retardant activity of the coated linen fabrics was improved as comparing to the uncoated linen fabric. In the flammability test, the char length varied from 48 to 41 mm, but the blank linen sample was completely burned. The organic ammonium polyphosphate flame retardant demonstrated to be washable for 24 cycles on linen fabrics. A greater concentration of aluminum strontium oxide nanoparticles doped with lanthanides enhanced the static contact angle from 147.1° to 153.7°, while reducing the sliding angle from 12 to 8°. When the density of phosphor nanoparticles on the linen surface was increased, a comparable increase in wettability time occurred. The air-permeability and bend-length of the treated

linen were found to be satisfactory and slightly affected by increasing the pigment nanoparticles on the fabric surface. The luminescent linen displayed a green emission at 519 nm upon excitation at 365 nm. To demonstrate the treated linen samples' glow in the dark, we left them in the dark for extended periods of time to show a significant greenish-yellow light emission. The current low-cost preparation strategy for linen fabrics with superhydrophobicity, ultraviolet protection, antimicrobial activity and flame-resistance, as well as long-persistent photoluminescence of high reversibility and photostability, could benefit high-performance functional textiles with functional properties.

Declarations

Acknowledgements

National Research Centre of Egypt is acknowledged for the financial support of the current research under project number (12010206).

Competing Interests

All the authors hereby declare that they do not have any conflict of interest about this manuscript.

Data Availability

All relevant data are within the manuscript and available from the corresponding author upon request.

Compliance with ethical standards

Conflict of interest

The authors declare that they have no conflict of interest.

Ethical approval

Not applicable.

Consent to participate

All authors were participated in this work.

Consent to publish

All authors agree to publish.

References

1. Liu H, Shen H, Zhang H, Wang X (2022) Development of photoluminescence phase-change microcapsules for comfort thermal regulation and fluorescent recognition applications in advanced

textiles. J Energy Storage 49:104158

2. Nascimento JHO, Felipe BHS, Dias JMTC, Souza AGF, Júnior APS, Galvão FMF, Cabral RLB, Carvalho BR (2021) Morais, and Awais Ahmad. "Creating Smart and Functional Textile Materials with Graphene". Nanomaterials and Nanotechnology. Springer, Singapore, pp 411–444
3. Hameed A, Aljuhani E, Bawazeer TM, Samar J, Almehmadi AA, Alfi HM, Abumelha (2021) Gaber AM Mersal, and Nashwa El-Metwaly. "Preparation of multifunctional long-persistent photoluminescence cellulose fibres." *Luminescence* 36, no. 7 : 1781–1792
4. Iyer S, Narayanan N, Behary V, Nierstrasz J, Guan, Chen G (2019) Study of photoluminescence property on cellulosic fabric using multifunctional biomaterials riboflavin and its derivative Flavin mononucleotide. Sci Rep 9(1):1–16
5. Wu Y, Gan J, Wu X (2021) Study on the silica-polymer hybrid coated SrAl2O4: Eu2+, Dy3 + phosphor as a photoluminescence pigment in a waterborne UV acrylic coating. J Mater Res Technol 13:1230–1242
6. Zhou C, Zhan P, Zhao J, Tang X, Liu W, Jin M, Wang X (2020) Long-lasting CaAl2O4: Eu2+, Nd3 + phosphor-coupled g-C3N4 QDs composites for the round-the-clock photocatalytic methyl orange degradation. Ceram Int 46(17):27884–27891
7. Li W, Liu Y, Ai P (2010) Synthesis and luminescence properties of red long-lasting phosphor Y2O2S: Eu3+, Mg2+, Ti4 + nanoparticles. Mater Chem Phys 119:1–2
8. Al-Qahtani SD, Adel M, Binyaseen E, Aljuhani M, Aljohani HK, Alzahrani R, Shah, Nashwa M (2022) El-Metwaly. "Production of smart nanocomposite for glass coating toward photochromic and long-persistent photoluminescent smart windows. Ceram Int 48(1):903–912
9. Khattab TA, Tolba E, Gaffer H, Samir Kamel (2021) Development of electrospun nanofibrous-walled tubes for potential production of photoluminescent endoscopes. Ind Eng Chem Res 60(28):10044–10055
10. Abumelha HM (2021) "Simple production of photoluminescent polyester coating using lanthanide-doped pigment." *Luminescence* 36, no. 4 : 1024–1031
11. Zhou Y, Ma Y, Sun Y, Xiong Z, Qi C, Zhang Y, Liu Y (2019) Robust superhydrophobic surface based on multiple hybrid coatings for application in corrosion protection. ACS Appl Mater Interfaces 11(6):6512–6526
12. Bake A, Merah N, Matin A, Gondal M, Qahtan T, Abu-Dheir N (2018) Preparation of transparent and robust superhydrophobic surfaces for self-cleaning applications. Prog Org Coat 122:170–179
13. Liravi M, Pakzad H, Moosavi A, Nouri-Borujerdi A (2020) A comprehensive review on recent advances in superhydrophobic surfaces and their applications for drag reduction. Prog Org Coat 140:105537
14. Manoharan K (2019) "Superhydrophobic surfaces review: Functional application, fabrication techniques and limitations. J Micromanufacturing 2(1):59–78
15. Parvate S, Dixit P (2020) "Superhydrophobic surfaces: insights from theory and experiment". J Phys Chem B 124(8):1323–1360

16. Sam E, Kobina DK, Sam X, Lv B, Liu X, Xiao S, Gong W, Yu (2019) Jie Chen, and Jun Liu. "Recent development in the fabrication of self-healing superhydrophobic surfaces. Chem Eng J 373:531–546
17. Jeevahan, Jeya M, Chandrasekaran G, Britto Joseph RB, Durairaj (2018) J. O. C. T. Mageshwaran. "Superhydrophobic surfaces: a review on fundamentals, applications, and challenges. J Coat Technol Res 15(2):231–250
18. Li A, Wang G, Ma Y, Zhao C, Zhang F, He Q, Zhang F (2021) Study on preparation and properties of superhydrophobic surface of RTV silicone rubber. J Mater Res Technol 11:135–143
19. Wang G, Li A, Li K, Zhao Y, Ma Y, He Q (2021) A fluorine-free superhydrophobic silicone rubber surface has excellent self-cleaning and bouncing properties. J Colloid Interface Sci 588:175–183
20. Zhou, Wei Y, Ma, He Q (2022) Investigation of self-cleaning and bouncing properties of superhydrophobic aluminum nitride/silicone rubber. J Appl Polym Sci 139(16):51990
21. Wang G, Li A, Zhao W, Xu Z, Ma Y, Zhang F, Zhang Y (2021) Jin Zhou, and Qiang He. "A review on fabrication methods and research progress of superhydrophobic silicone rubber materials. Adv Mater Interfaces 8(1):2001460
22. He W, Song P, Yu B, Fang Z, Wang H (2020) Flame retardant polymeric nanocomposites through the combination of nanomaterials and conventional flame retardants. Prog Mater Sci 114:100687
23. Xu Y-J, Qu L-Y, Liu Y, Zhu P (2021) An overview of alginates as flame-retardant materials: Pyrolysis behaviors, flame retardancy, and applications. Carbohydr Polym 260:117827
24. Nabipour H, Wang X, Song L, Yuan, Hu (2020) Metal-organic frameworks for flame retardant polymers application: A critical review. Compos Part A: Appl Sci Manufac 139:106113
25. Li Y-M (2020) "Polymer-based ceramifiable composites for flame retardant applications: A review. Compos Commun 21:100405
26. Caringella R, Patrucco A, Simionati M, Gavignano S, Montarsolo A, Mossotti R, Zoccola M, Tonin C, Fabris R, Floria L (2018) "Electrically conducting linen fabrics for technical applications". Text Res J 88(2):144–154
27. He X, Liu Q, Wang J, Chen H (2019) Wearable gas/strain sensors based on reduced graphene oxide/linen fabrics. Front Mater Sci 13(3):305–313
28. Wang Y, Miao M (2021) Helical shape linen artificial muscles responsive to water. Smart Mater Struct 30(7):075031
29. Teli MD, Pandit P (2018) A novel natural source Sterculia foetida fruit shell waste as colorant and ultraviolet protection for linen. J Nat Fibers 15(3):337–343
30. Liang Jing-jing, Zhao Zong-bin, Tang Yong-chao, Liang Zhi-hui, Xin LS, Pan (2020) Xu-zhen Wang, and Jie-shan Qiu. "A wearable strain sensor based on carbon derived from linen fabrics. New Carbon Mater 35(5):522–530
31. Liu J, Lv C (2021) Synthesizing environmentally friendly non-silicone oxygen bleaching stabilizer for linen yarn using oligomeric acrylic acid. Sci Rep 11(1):1–11

32. Binyaseen AM, Bayazeed A, Samar Y, Al-nami KA, Al-Ola SA, Alqarni, Shams H, Abdel-Hafez, Nashwa M, El-Metwaly (2022) Development of epoxy/rice straw-based cellulose nanowhiskers composite smart coating immobilized with rare-earth doped aluminate: Photoluminescence and anticorrosion properties for sustainability. Ceram Int 48(4):4841–4850
33. Jiang D, Bin X, Liu Y, Yuan L, Feng J, Ji J, Wang D, Losic H-C (2020) Yao, and Yu Xin Zhang. "Biotemplated top-down assembly of hybrid Ni nanoparticles/N doping carbon on diatomite for enhanced catalytic reduction of 4-nitrophenol". Chem Eng J 383:123156
34. Atta AM (2021) "Immobilization of silver and strontium oxide aluminate nanoparticles integrated into plasma-activated cotton fabric: luminescence, superhydrophobicity, and antimicrobial activity." *Luminescence* 36, no. 4 : 1078–1088
35. Wongphan P (2020) "Characterization of starch, agar and maltodextrin blends for controlled dissolution of edible films. Int J Biol Macromol 156:80–93
36. Horrocks A, Richard A, Sitpalan, Baljinder K (2019) Kandola. "Design and characterisation of bicomponent polyamide 6 fibres with specific locations of each flame retardant component for enhanced flame retardancy. Polym Test 79:106041
37. Shin Y, Son K, Yoo DI (2010) Development of natural dyed textiles with thermo-regulating properties. Thermochimica acta 511(1–2):1–7
38. Zhou X, Song W, Zhu G (2020) "A facile approach for fabricating silica dioxide/reduced graphene oxide coated cotton fabrics with multifunctional properties." *Cellulose* 27, no. 5 : 2927–2938
39. Katouah H, El-Metwaly NM (2021) Plasma treatment toward electrically conductive and superhydrophobic cotton fibers by in situ preparation of polypyrrole and silver nanoparticles. Reactive and Functional Polymers 159:104810
40. Khattab TA, Moustafa MG, Fouda MS, Abdelrahman, Sarah I, Othman, Ahmed A (2019) Allam. "Development of illuminant glow-in-the-dark cotton fabric coated by luminescent composite with antimicrobial activity and ultraviolet protection." *Journal of fluorescence* 29, no. 3 : 703–710
41. Mishra VR, Chaitannya W, Ghanavatkar, Sekar N (2019) UV protective heterocyclic disperse azo dyes: Spectral properties, dyeing, potent antibacterial activity on dyed fabric and comparative computational study. Spectrochim Acta Part A Mol Biomol Spectrosc 223:117353
42. Ahmed N, Ahmed R, Rafiqe M, Baig MA (2017) A comparative study of Cu–Ni alloy using LIBS, LA-TOF, EDX, and XRF. Laser Part Beams 35(1):1–9
43. Khattab TA, Mowafi S, El-Sayed H (2019) "Development of mechanically durable hydrophobic lanolin/silicone rubber coating on viscose fibers." *Cellulose* 26, no. 17 : 9361–9371
44. Al-Qahtani S, Aljuhani E, Felaly R, Alkhamis K, Alkabli J (2021) Alaa Munshi, and Nashwa El-Metwaly. "Development of photoluminescent translucent wood toward photochromic smart window applications. Ind Eng Chem Res 60(23):8340–8350.

Figures

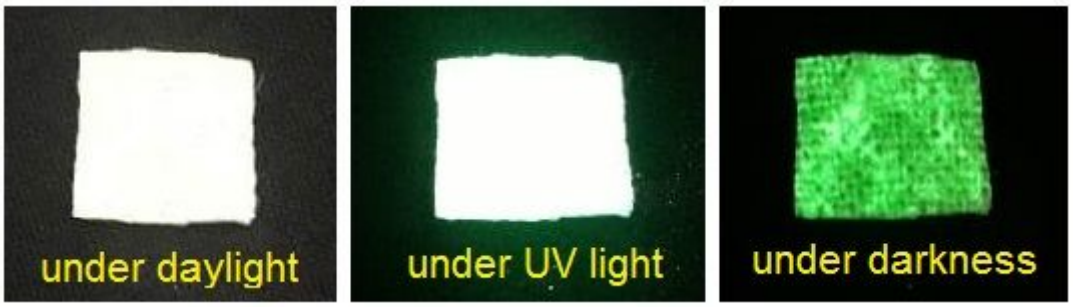

Figure 1

Photographs of $LSAO_7$ under daytime light (a), UV rays (b), and complete darkness (c).

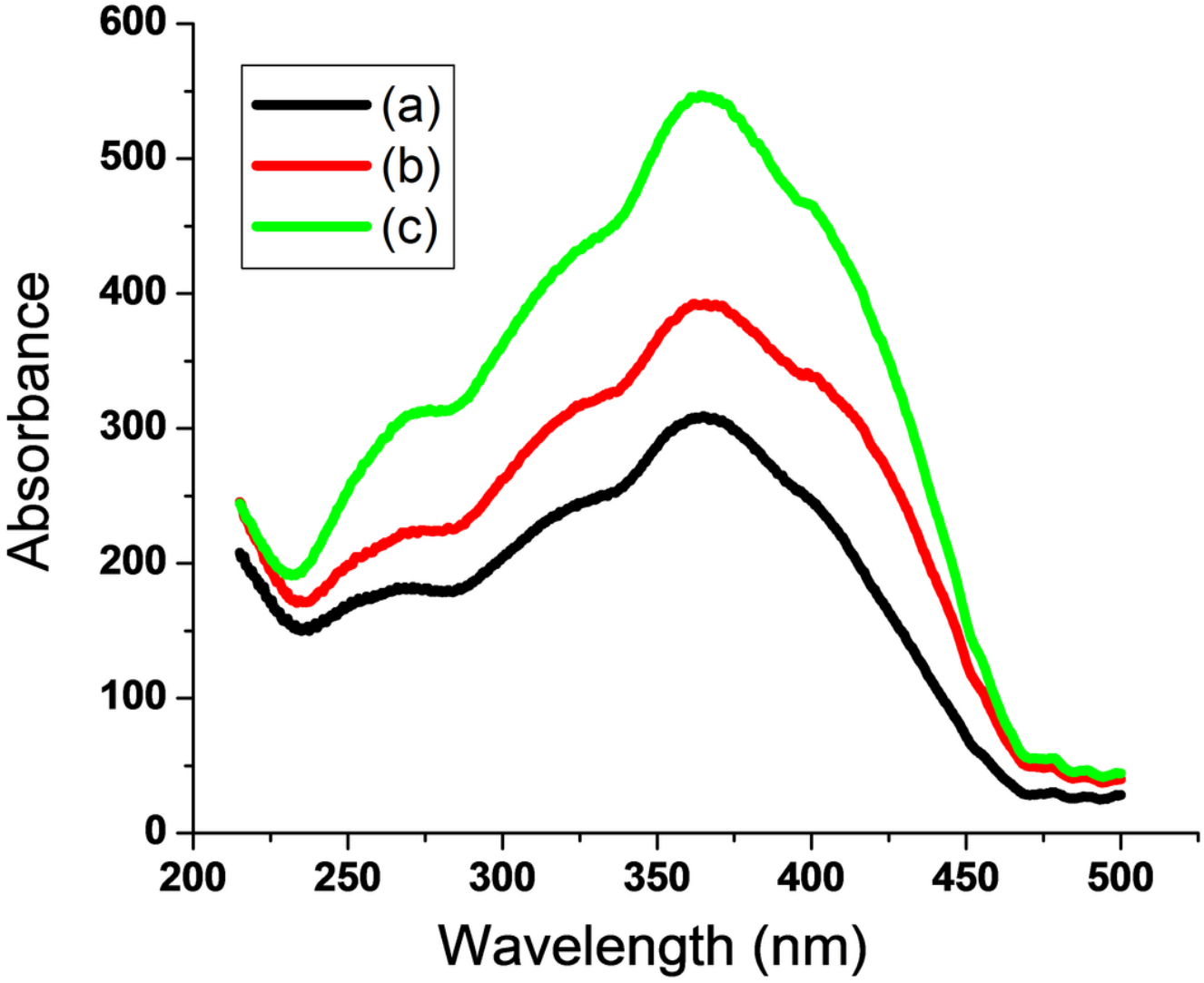

Figure 2

Excitation spectra of $LSAO_7$.

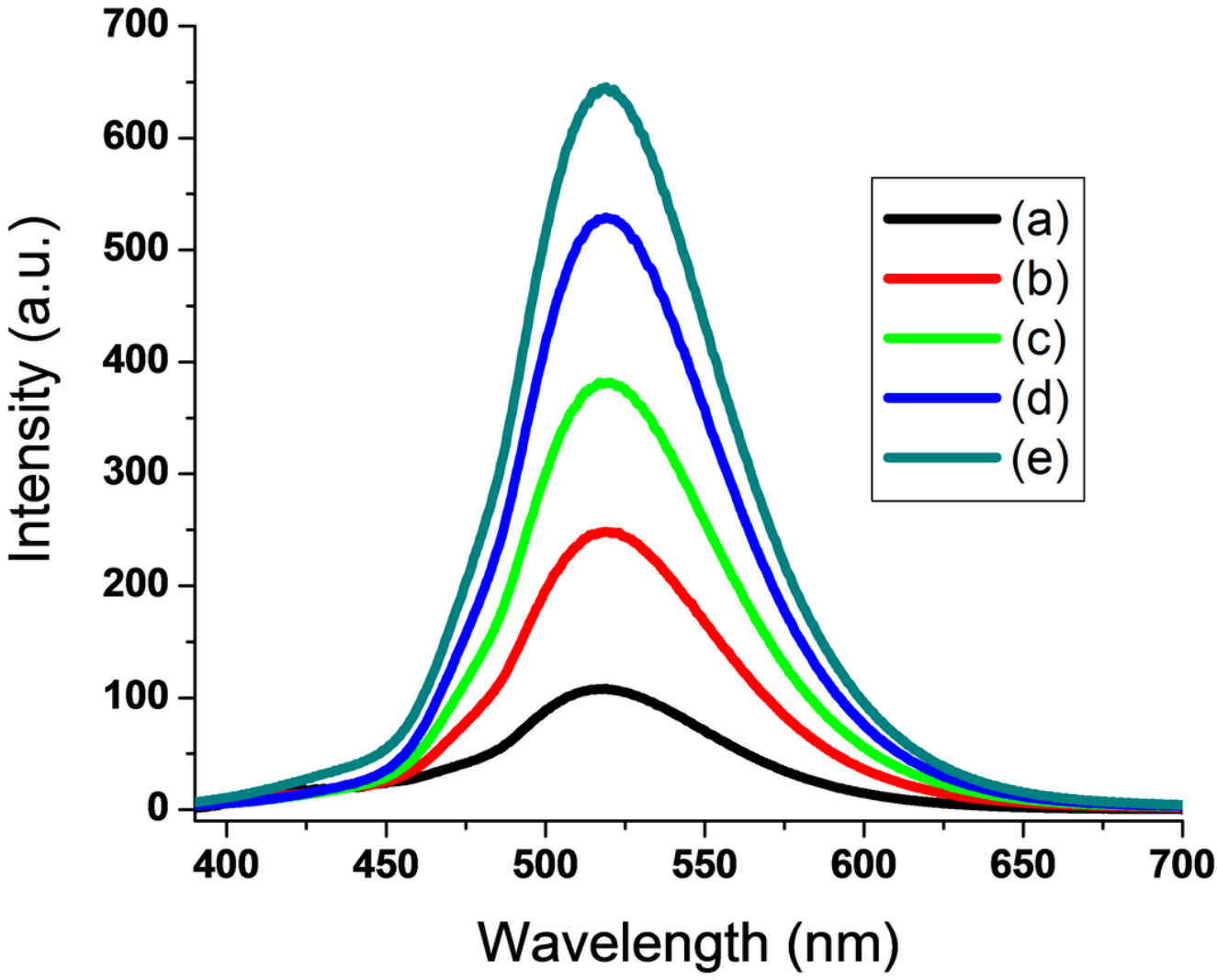

Figure 3

Emission spectra of $LSAO_7$.

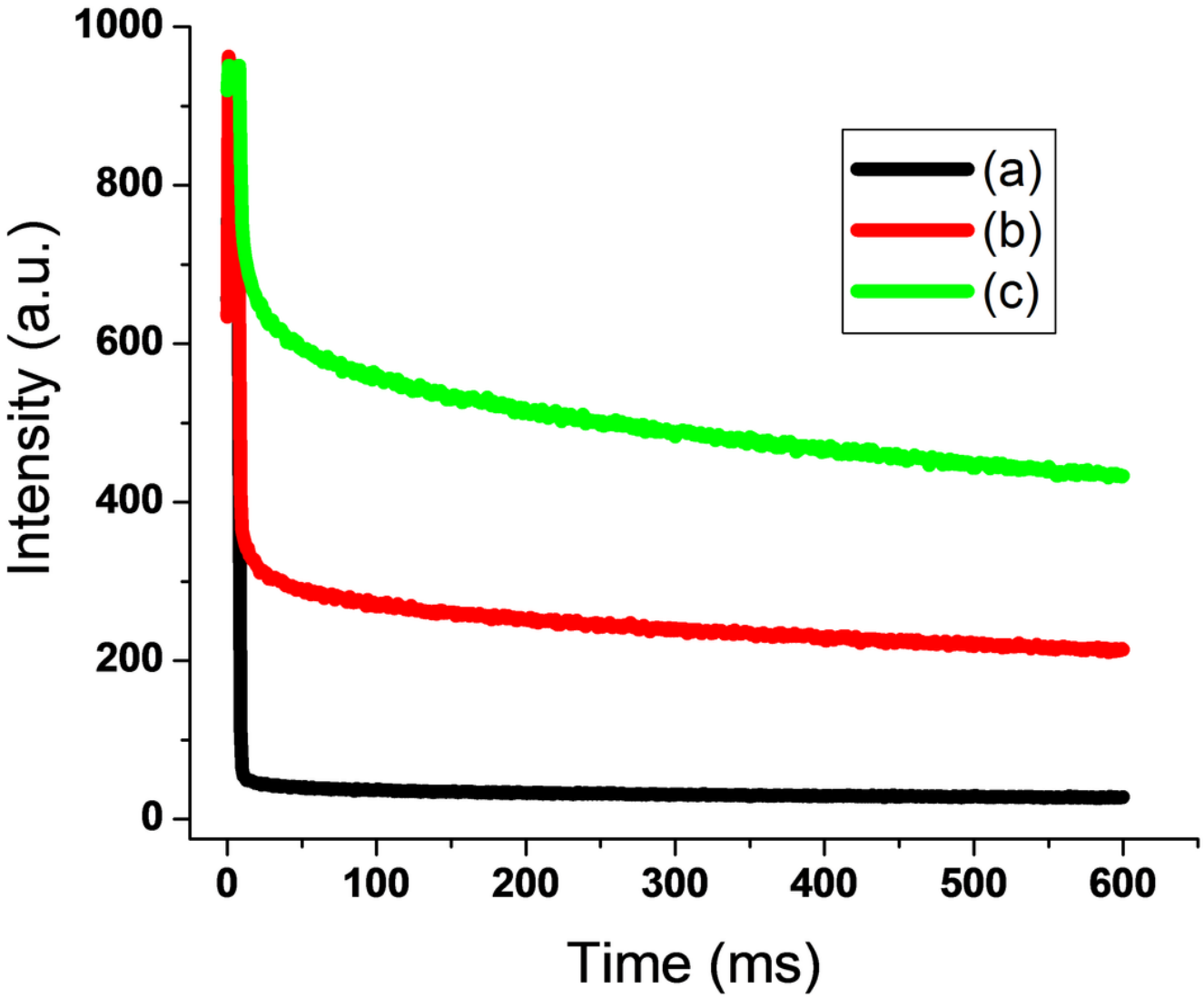

Figure 4

Lifetime spectrum of $LSAO_7$.

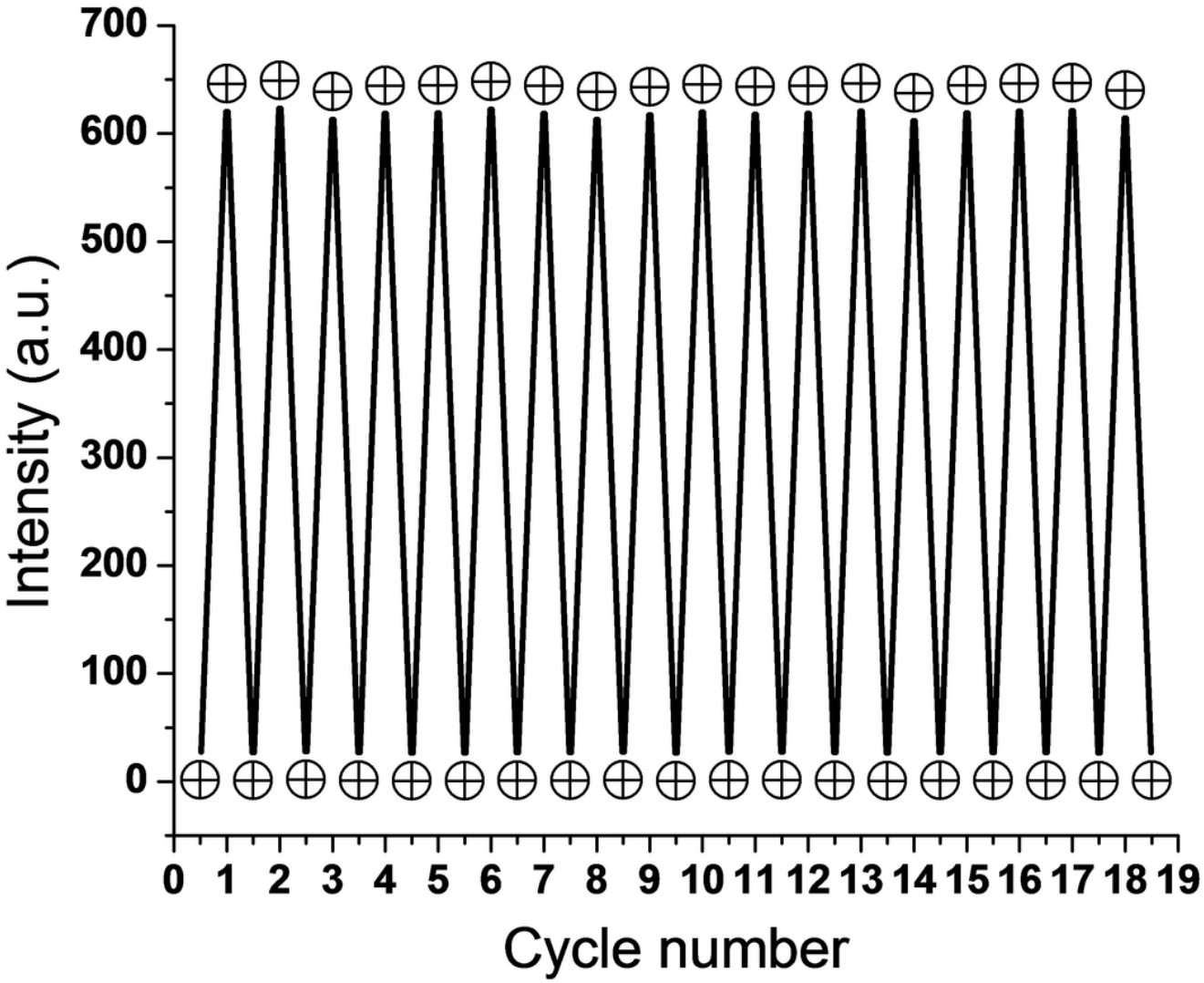

Figure 5

Photostability of $LSAO_7$ linen fabric at 519 nm.

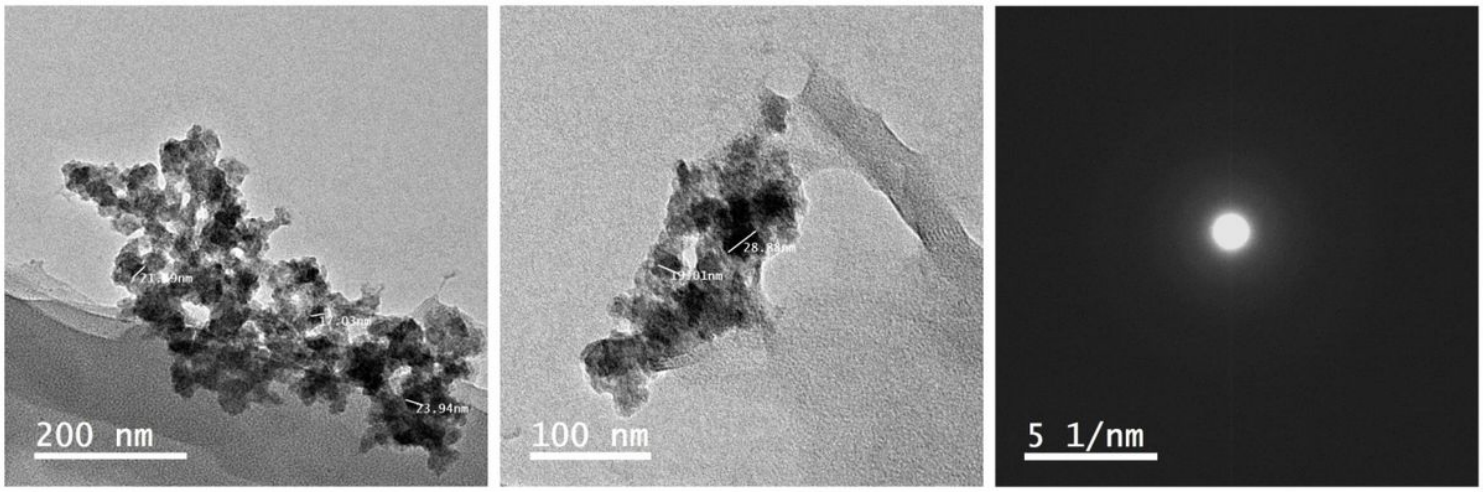

Figure 6

TEM micrographs of LSAO *nanoscale particles.*

Figure 7

SEM images of coated linen.

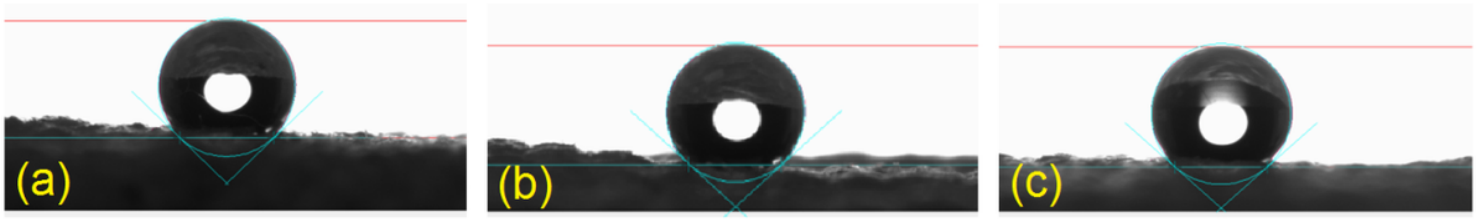

Figure 8

Static Contact angles of treated linen; $LSAO_1$ (a), $LSAO_9$ (b), and $LSAO_7$ (c).

Figure 9

Effect of laundry cycles on flammability of linen.